Computational study on the role of residue Arg166 in alkaline phosphatases

Gabriela L. Borosky

*INFIQC, CONICET and Departamento de Química Teórica y Computacional, Facultad de Ciencias Químicas,
Universidad Nacional de Córdoba, Ciudad Universitaria, Córdoba 5000, Argentina
E-mail: gborosky@fcq.unc.edu.ar*

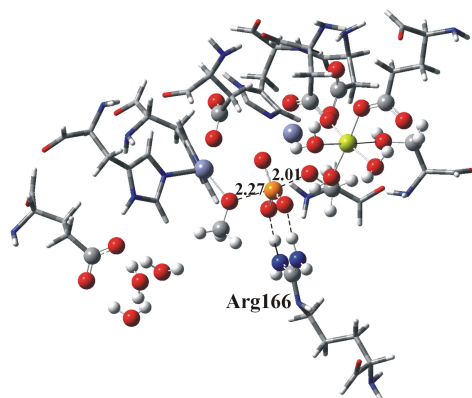Dedicated to Prof. Kenneth K. Laali on the occasion of his 65th birthday
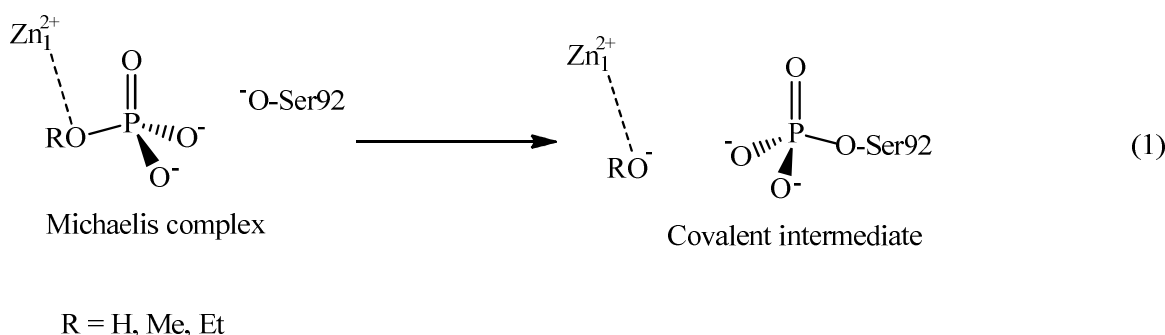
Abstract

Quantum chemical calculations were performed with the goal of achieving a better understanding of the influence of Arg166 on the catalytic activity of alkaline phosphatases. The present results indicate that the active site Arg166 residue contributes to catalysis by orienting the phosphate monoester substrate in a favorable position for the rate-limiting nucleophilic attack. The stabilizing hydrogen bond interactions of the guanidinium group with two nonbridging oxygens of the phosphate decrease the barrier for the phosphoryl transfer process by attainment of a tighter and preorganized transition state.

Keywords: Enzymatic catalysis, quantum mechanics, ONIOM calculations, phosphoryl transfer

Introduction

Alkaline phosphatases (APs) comprise a large family of metalloenzymes present in nearly all living species.[1] As the amino acid sequence of APs from different organisms is remarkably conserved, particularly residues in the active site and surrounding regions,[2,3] the catalytic mechanism determined for the *E. coli* bacterial enzyme has been proposed to be analogous for eukaryotic APs.[4] These enzymes catalyze the hydrolysis and transphosphorylation of phosphate monoesters, with formation of a covalent phosphoserine intermediate and release of inorganic phosphate and an alcohol.[5] Kinetic and biochemical data have suggested a two-step reaction catalytic mechanism (Scheme 1).[6-8] The first chemical step involves generation of the covalent intermediate E-P (k_2, Scheme 1), and this phosphoserine is hydrolyzed in the second chemical step (k_3, Scheme 1). Transphosphorylation to a phosphate acceptor (k_5, Scheme 1) occurs in nucleophilic buffers (presence of $R^{'}OH$).

$$E + ROP \underset{k_{-1}}{\overset{k_1}{\rightleftharpoons}} E{\cdot}ROP \xrightarrow{k_2} E\text{-}P$$

$P = PO_3{}^{2-}$

$$E{\cdot}ROP \xrightarrow{k_2} E\text{-}P \quad (ROH)$$

$$H_2O \underset{k_{-3}}{\overset{k_3}{\rightleftharpoons}} E{\cdot}P_i \xrightarrow{k_4} E + P_i$$

$$R^{'}OH \underset{k_{-5}}{\overset{k_5}{\rightleftharpoons}} E{\cdot}R^{'}OP \xrightarrow{k_6} E + R^{'}OP$$

Scheme 1. Catalytic mechanism of APs.

Many enzymes that catalize phosphoryl transfer reactions contain arginine residues in their active sites. Mutagenesis studies have found that loss of the arginine side chain causes a notable reduction in catalysis. Mutation of the residue arginine 166 in *E. coli* AP to serine, alanine or lysine decreases the rate of hydrolysis of phosphate monoesters; this effect was suggested to be ascribed to specific stabilizing interactions of arginine with the charge and/or geometry of the transition state for phosphoryl transfer.[9]

Computational methods were recently applied to study the hydrolysis of phosphate esters within the active site of human placental AP (PLAP) as a model AP.[10-12] These calculations provided interesting insights regarding the catalytic mechanism of this family of enzymes. In this work, quantum mechanical calculations were performed with the aim of achieving a better understanding of the influence of Arg166 on the catalytic activity of APs. For validation purposes, the present theoretical results were compared with experimental studies reported in the literature.

Results and Discussion

The first chemical step of the catalytic mechanism of APs, which is formation of the covalent phosphoserine intermediate via nucleophilic attack of the catalytic Ser92 (k_2, Scheme1), was study computationally (Reaction 1). This process was evaluated in the active site of PLAP, as well as within the Arg166Ser mutant protein, in

which the amino acid Arg166 was replaced by serine. This reaction step has been determined as rate-limiting for the enzymatic hydrolysis of alkyl phosphates.[10-13] Calculations were performed for hydrogen, methyl, and ethyl phosphate dianions as substrates. Computed energy changes are shown in Table 1, and the structures of stationary points are illustrated in Figure 1.

$$Zn_1^{2+} \quad \cdots \quad \begin{matrix} O \\ \| \\ RO-P^{''''}O^- \\ | \\ O^- \end{matrix} \quad {}^-O\text{-Ser92} \quad \longrightarrow \quad Zn_1^{2+} \quad \cdots \quad RO^- \quad {}^-O^{''''}\begin{matrix} O \\ \| \\ P-O\text{-Ser92} \\ | \\ O^- \end{matrix} \qquad (1)$$

Michaelis complex   Covalent intermediate

R = H, Me, Et

The initial coordinates for the respective Michaelis complexes had been determined by previous molecular docking calculations.[10,12] In this complexes, the oxygen of the ester leaving group was coordinated to Zn_1, and one nonbridging oxygen was coordinated to Zn_2 (Figure 1a). In the case of PLAP, the other two nonbridging oxygen atoms formed hydrogen bond interactions with the guanidinium group of Arg166 (the average O-H distances being 1.52 Å and 1.64 Å), and with a Mg_3-bound water. For the Arg166Ser mutant, the lack of stabilizing interactions with Arg166 caused a rotation in the position of the phosphate group to achieve an additional hydrogen bond with a second Mg_3-bound water molecule; the hydroxylic hydrogen of Ser166 was *ca.* 5.56 Å away from the nearest phosphate oxygen. These observations match exactly with the X-ray crystallographic structures for noncovalently bound inorganic phosphate in the wild-type enzyme and Arg166Ser mutant.[9]

Transition states (TSs) presented a trigonal bipyramidal configuration corresponding to an in-line displacement reaction, as proposed by Holtz *et al.*,[14] with bond forming/breaking oxygens in an opposite axial disposition (Figure 1b). In all cases, departure of the leaving group was assisted by coordination with Zn_1. The three nonbridging oxygens of the transferring phosphoryl group bisected the axial plane and formed stabilizing interactions with Zn_2 and one Mg_3-bound water, and, in the active site of PLAP, also with Arg166. Interactions of the nonbridging phosphoryl oxygens with the residue Arg166 in PLAP generated tighter TSs than in the case of Arg166Ser, with shorter forming/breaking bonds between the phosphorus atom and the nucleophile and leaving group oxygens (Table 2).

Table 1. Computed activation energies for Reaction 1 (experimentally estimated values in parenthesis)

Substrate	$\Delta E^{\neq}$ (kcal/mol)	
	PLAP	**Arg166Ser**
Hydrogen phosphate	20.8 (20.5[a])	21.7 (21.7[a])
Methyl phosphate	16.1 (9.2,[b] 9.9[c])	16.7 (14.7,[d] 15.1[c])
Ethyl phosphate	17.5 (10.4[b])	17.9 (15.6[d])

[a] Reference 9 (calculated from k_{cat} (s^{-1})). [b] Reference 13 (calculated from k_{cat}/K_M (M.s^{-1})). [c] Reference 26 (calculated from k_{cat}/K_M (M.s^{-1})). [d] Reference 9 (calculated from k_{cat}/K_M (M.s^{-1})).
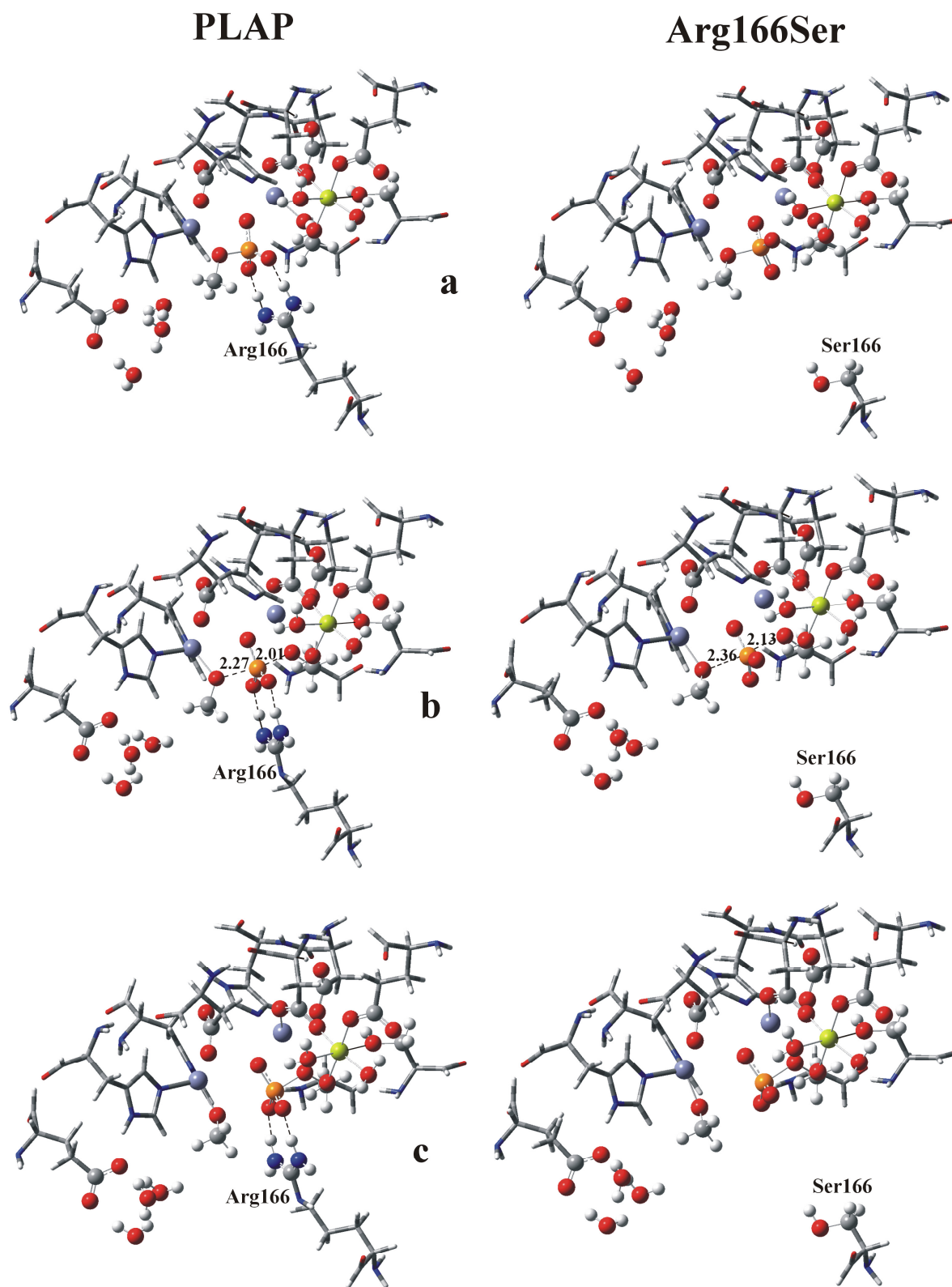
PLAP　　　　　　　　　　　　　　　　**Arg166Ser**

Figure 1. Stationary points: (a) Michaelis complexes; (b) TSs (bond lengths in Å); (c) Covalent intermediates.

Table 2. Relevant bond distances in the characterized TSs (Å)[a]

Substrate	PLAP		Arg166Ser	
	P-O_{nu}	P-O_{lg}	P-O_{nu}	P-O_{lg}
Hydrogen phosphate	2.002	2.256	2.146	2.350
Methyl phosphate	2.011	2.275	2.131	2.361
Ethyl phosphate	2.028	2.257	2.153	2.345

[a] O_{nu}: oxygen atom of the nucleophilic Ser92 residue; O_{lg}: oxygen atom of the leaving group.

It should be noticed that hydrogen bonds between the phosphate oxygens and Arg166 were not stronger in the TSs than in their respective Michaelis complexes. Moreover, TS stabilization by Arg166 did not involved an increase in electrostatic stabilization of the phosphoryl group by the Zn^{2+} ions, which would imply shorter distances between one nonbridging oxygen and these cations. Instead, Arg166 appears to decrease the activation energy for covalent phosphoserine formation by orienting the phosphate group to a preorganized arrangement that gives rise to a tighter and lower-energy TS.

In order to test the accuracy of the theoretical procedures applied, the present computational results were contrasted with experimental assessments available in the literature. It is important to note that comparison of theoretical and experimental kinetic data is not straightforward. Computed barriers correspond to the energy difference between the TS and the Michaelis complex and are related to k_{cat}. On the other hand, experimental values are usually reported as k_{cat}/K_M, which provide barriers measured from the ground state of the free enzyme and substrate in solution to the TS for the first irreversible reaction step. As both barriers differ by the binding energy of the substrate (an exothermic process), activation energies derived from experimental k_{cat}/K_M values correspond to lower bounds of the calculated barriers.

The activation energies yielded by the calculations in this work and the corresponding experimental evaluations[9,13] (barriers were derived from k_{cat} and k_{cat}/K_M values by transition-state theory[15]) are presented in Table 1. It is worth noting the remarkably accordance between both energy barriers computed for $HOPO_3^{2-}$ and those resulting from experimental k_{cat} estimations. Moreover, computed activation barriers were higher than those derived from k_{cat}/K_M values, supporting the reliability of the computational methodology employed.

The present calculations indicate a reduction in the catalytic efficiency of the Arg166Ser mutant enzyme as compared to wild-type PLAP, in agreement with previous experimental results (Table 1). The characterized stationary points revealed hydrogen bonding contacts between the guanidinium group of the Arg166 residue and two nonbridging oxygens of the phosphate. In this way, Arg166 places the phosphate group of the substrate closer to the catalytic Ser92 and in a proper orientation for nucleophilic attack. These hydrogen bond interactions are conserved across the whole reaction coordinate, and lower the barrier height of the rate-determining phosphoryl transfer by further stabilizing the corresponding TS. Consistent with this, in the presence of Arg166 the located TSs structures exhibited shorter forming/breaking bonds between P and the O atoms of the nucleophile and leaving group.

Conclusions

The active site Arg166 residue in APs enhances the activity of this family of enzymes by locating the phosphate monoester substrates in a more favorable position for the rate-limiting nucleophilic attack. The stabilizing

hydrogen bond interactions with the guanidinium group decrease the barrier of the phosphoryl transfer process by generating a more compact and preorganized TS. The present computational results are in very good accordance with X-ray crystallographic structures and experimental kinetic data, which supports the mechanistic observations inferred from this theoretical study.

Computational Methods

The three-dimensional structure of PLAP was obtained from the Protein Data Bank (PDB code 1EW2).[16] The computational model contained the catalytic metal triad (two Zn^{2+} ions (M1 and M2) and one Mg^{2+} ion (M3)) with their ligands Asp316, His320, His432, His358, Asp357, Asp42, Glu311, Ser155, and the nucleophilic Ser92, as well as residues Arg166 and Glu429. Valences at cut peptide bonds were completed with hydrogen atoms. Three water molecules to complete Mg^{2+} coordination (one as a hydroxide ion), and three more coordinated to Glu429 were included. Ionized side chains were defined for arginine, aspartate, and glutamate residues; histidines were neutral and singly protonated on Hδ. The complete model system had a net charge of -1, consisting of seven positive charges (two Zn^{2+} cations, one Mg^{2+}, and one arginine) and eight negative charges (three aspartates, two glutamates, one hydroxide anion, and the phosphate monoester dianion substrate). The Arg166Ser mutant was built by replacing the side chain of Arg166 by a serine; therefore, this protein model had a total charge equal to -2.

The Gaussian 09 package[17] was employed to carry out ONIOM[18] calculations using two quantum-mechanical layers (QM:QM). Density Functional Theory (DFT) geometry optimizations with the B3LYP[19-21] functional were performed for the high layer, containing the three metal cations, the phosphate monoester dianions, five water molecules, one hydroxide ion, carboxylate groups of glutamates and aspartates, -CH_2OH groups of serines, and the -$C(NH_2)_2$ group of arginine (around 40 heavy atoms and 25 hydrogens). The 6-31+G* basis set was used for C, O, N, P, Mg and H atoms, and the pseudopotential Lanl2DZ was applied for Zn cations. The low layer (about 73 heavy atoms and 78 hydrogens) was treated with the semi-empirical method PM3MM.[22] This ONIOM(B3LYP:PM3MM) methodology has been verified to be suitable in our prior studies.[10-12] The electrostatic effect of the environment was taken into account by polarized continuum model (IEFPCM)[23] optimizations, considering a dielectric constant ε = 4.0 to simulate the influence of the residues surrounding the active site. The positions of backbone atoms involved in peptide bonds were fixed to conserve the active site structure, and the coordinates of the rest of the atoms were fully optimized. Harmonic vibrational frequency calculations were performed to confirm the nature of the minima and TSs on the potential energy surfaces. Intrinsic reaction coordinate (IRC)[24,25] calculations were also employed to verify TSs. Although the accuracy of the energies was not affected, the harmonic entropy effects were inaccurate due to the presence of constrained atoms. These approximations did not perturb the comparison of activation free energies between different substrates in the same protein. However, as two different enzymes were considered in the current study, the zero-point energy and entropic corrections were not included in the calculated barriers. ONIOM(B3LYP/6-311+G(2d,p):PM3MM)-IEFPCM single points were computed on the optimized stationary points to get more precise energies.

A very similar methodology was also validated in recent computational studies involving the hydrolysis of a phosphate group by a protein phosphatase,[27] and the hydrolysis mechanisms of trimethyl phosphate and its resulting phosphodiester by a phosphotriesterase.[28]

Acknowledgements

References and Notes

1. McComb, R. B.; Bowers, G. N., Jr.; Posen, S. In *Alkaline Phosphatases*; Plenum Press: New York, 1979; pp 986-989.
   https://doi.org/10.1007/978-1-4613-2970-1
2. Kim, E. E.; Wyckoff, H. W. *Clin. Chim. Acta* **1990**, *186*, 175-178.
   https://doi.org/10.1016/0009-8981(90)90035-Q
3. Murphy, J. E.; Tibbitts, T. T.; Kantrowitz, E. R. *J. Mol. Biol.* **1995**, *253*, 604-617.
   https://doi.org/10.1006/jmbi.1995.0576
4. Kim, E. E.; Wyckoff, H. W. *J. Mol. Biol.* **1991**, *218*, 449-464.
   https://doi.org/10.1016/0022-2836(91)90724-K
5. Schwartz, J. H.; Lipmann, F. *Proc. Natl. Acad. Sci. USA* **1961**, *47*, 1996-2005.
   https://doi.org/10.1073/pnas.47.12.1996
6. Holtz, K. M.; Kantrowitz, E. R. *FEBS Lett.* **1999**, *462*, 7-11.
   https://doi.org/10.1016/S0014-5793(99)01448-9
7. Reid, T. W.; Wilson, I. B. In *The Enzymes*; Boyer, P. D., Ed.; Academic Press: New York, 1971; Vol. 4, pp 373-415.
8. Coleman, J. E. *Annu. Rev. Biophys. Biomol. Struct.* **1992**, *21*, 441-483.
   https://doi.org/10.1146/annurev.bb.21.060192.002301
9. O´Brien, P. J.; Lassila, J. K.; Fenn, T. D.; Zalatan, J. G.; Herschlag, D. *Biochemistry* **2008**, *47*, 7663-7672 and references cited therein.
   https://doi.org/10.1021/bi800545n
10. Borosky, G. L.; Lin, S. *J. Chem. Inf. Model.* **2011**, *51*, 2538-2548.
    https://doi.org/10.1021/ci200228s
11. Borosky, G. L. *J. Phys. Chem. B* **2014**, *118*, 14302-14313.
    https://doi.org/10.1021/jp511221c
12. Borosky, G. L. *J. Chem. Inf. Model.* **2017**, *57*, 540-549.
    https://doi.org/10.1021/acs.jcim.6b00755
13. O´Brien, P. J.; Herschlag, D. *Biochemistry* **2002**, *41*, 3207-3225.
    https://doi.org/10.1021/bi012166y
14. Holtz, K. M.; Stec, B.; Kantrowitz, E. R. *J. Biol. Chem.* **1999**, *274*, 8351-8354.
    https://doi.org/10.1074/jbc.274.13.8351
15. Classical transition-state theory expresses the rate constant for a reaction as $k = (k_B T/h)\exp(-\Delta G^{\neq}/RT)$, in which k_B is the Boltzmann constant, R is the gas constant, T is the absolute temperature, h is the Planck constant, and $\Delta G^{\neq}$ is the free energy of activation.

16. Le Du, M. H.; Stigbrand, T.; Taussig, M. J.; Ménez, A.; Stura, E. A. *J. Biol. Chem.* **2001**, *276*, 9158-9165.
https://doi.org/10.1074/jbc.M009250200

17. Frisch, M. J.; Trucks, G. W.; Schlegel, H. B.; Scuseria, G. E.; Robb, M. A.; Cheeseman, J. R.; Montgomery, Jr., J. A.; Vreven, T.; Kudin, K. N.; Burant, J. C.; Millam, J. M.; Iyengar, S. S.; Tomasi, J.; Barone, V.; Mennucci, B.; Cossi, M.; Scalmani, G.; Rega, N.; Petersson, G. A.; Nakatsuji, H.; Hada, M.; Ehara, M.; Toyota, K.; Fukuda, R.; Hasegawa, J.; Ishida, M.; Nakajima, T.; Honda, Y.; Kitao, O.; Nakai, H.; Klene, M.; Li, X.; Knox, J. E.; Hratchian, H. P.; Cross, J. B.; Bakken, V.; Adamo, C.; Jaramillo, J.; Gomperts, R.; Stratmann, R. E.; Yazyev, O.; Austin, A. J.; Cammi, R.; Pomelli, C.; Ochterski, J. W.; Ayala, P. Y.; Morokuma, K.; Voth, G. A.; Salvador, P.; Dannenberg, J. J.; Zakrzewski, V. G.; Dapprich, S.; Daniels, A. D.; Strain, M. C.; Farkas, O.; Malick, D. K.; Rabuck, A. D.; Raghavachari, K.; Foresman, J. B.; Ortiz, J. V.; Cui, Q.; Baboul, A. G.; Clifford, S.; Cioslowski, J.; Stefanov, B. B.; Liu, G.; Liashenko, A.; Piskorz, P.; Komaromi, I.; Martin, R. L.; Fox, D. J.; Keith, T.; Al-Laham, M. A.; Peng, C. Y.; Nanayakkara, A.; Challacombe, M.; Gill, P. M. W.; Johnson, B.; Chen, W.; Wong, M. W.; Gonzalez, C.; Pople, J. A. *Gaussian 09*, Revision E.01; Gaussian, Inc.: Wallingford, CT, 2009.

18. Dapprich, S.; Komáromi, I.; Byun, K. S.; Morokuma, K.; Frisch, M. J. *J. Mol. Struct. (Theochem)* **1999**, *461-462*, 1–21.
https://doi.org/10.1016/S0166-1280(98)00475-8

19. Becke, A. D. *J. Chem. Phys.* **1993**, *98*, 5648-5652.
https://doi.org/10.1063/1.464913

20. Lee, C.; Yang, W.; Parr, R. G. *Physical Review B* **1988**, *37*, 785-789.
https://doi.org/10.1103/PhysRevB.37.785

21. Miehlich, B.; Savin, A.; Stoll, H.; Preuss, H. *Chem. Phys. Lett.* **1989**, *157*, 200-206.
https://doi.org/10.1016/0009-2614(89)87234-3

22. Stewart, J. J. P. *J. Comp. Chem.* **1989**, *10*, 209-220.
https://doi.org/10.1002/jcc.540100208

23. Tomasi, J.; Mennucci, B.; Cancès, E. *J. Mol. Struct. (Theochem)* **1999**, *464*, 211-226.
https://doi.org/10.1016/S0166-1280(98)00553-3

24. Fukui, K. *Acc. Chem. Res.* **1981**, *14*, 363-68.
https://doi.org/10.1021/ar00072a001

25. Hratchian, H. P.; Schlegel, H. B. In *Theory and Applications of Computational Chemistry: The First 40 Years*; Dykstra, C. E.; Frenking, G.; Kim, K. S.; Scuseria, G. Eds.; Elsevier: Amsterdam, 2005; pp 195-249.
https://doi.org/10.1016/B978-044451719-7/50053-6

26. Sunden, F.; Peck, A.; Salzman, J.; Ressl, S.; Herschlag, D. *eLife* **2015**, *4*, e06181.
https://doi.org/10.7554/eLife.06181

27. Ribeiro, A. J. M.; Alberto, M. E.; Ramos, M. J.; Fernandes, P. A.; Russo, N. *Chem. Eur. J.* **2013**, *19*, 14081-14089.
https://doi.org/10.1002/chem.201301565

28. Alberto, M. E.; Pinto, G.; Russo, N.; Toscano, M. *Chem. Eur. J.* **2015**, *21*, 3736-3745.
https://doi.org/10.1002/chem.201405593